EGFR activity upregulates lactate dehydrogenase A (LDHA) expression, LDH activity, and lactate secretion in cultured IB3-1 cystic fibrosis lung epithelial cells

María Macarena Massip-Copiz, Ángel G. Valdivieso, Mariángeles Clauzure[1], Consuelo Mori, Cristian J. A. Asensio, María Á. Aguilar and Tomás A. Santa-Coloma*

From the Laboratory of Cellular and Molecular Biology, Institute for Biomedical Research (BIOMED), School of Medical Sciences, Pontifical Catholic University of Argentina (UCA), and the National Scientific and Technical Research Council of Argentina (CONICET), Buenos Aires, Argentina.

[1]At present in the Faculty of Veterinary Science, National University of La Pampa (UNLPam), Argentina.

Running tittle: EGFR and extracellular pH in IB3-1 CF cells

*To whom correspondence should be addressed: Tel/Fax: 5411-4338-0886, E-mail: tsantacoloma@gmail.com, tomas_santacoloma@uca.edu.ar. Address: Tomás A. Santa Coloma, Laboratory of Cellular and Molecular Biology, Institute for Biomedical Research, School of Medical Sciences, Pontifical Catholic University of Argentina, Alicia Moreau de Justo 1600, 3rd Floor, Buenos Aires, C1107AFF, Argentina.

ABSTRACT

Cystic fibrosis (CF) is caused by mutations in the CFTR gene. It has been postulated that a reduced HCO_3^- transport in CF through CFTR may lead to a decreased airway surface liquid (ASL) pH. In contrast, others have reported no changes in the extracellular pH (pHe). We have recently reported that in carcinoma Caco-2/pRS26 cells (shRNA for CFTR) or CF lung epithelial IB3-1 cells, the CFTR failure decreased mitochondrial Complex I activity due to an autocrine IL1B loop, and increased lactic acid production. The secreted lactate accounted for the reduced pHe since oxamate fully restored the pHe. These effects were attributed to the IL-1β autocrine loop and the downstream signaling kinases c-Src and JNK. Here we show that the pHe of IB3-1 cells can be restored to normal pHe values (~7.4) by incubation with the epidermal growth factor receptor (EGFR, HER1, ErbB1) inhibitors AG1478 or PD168393. The inhibitor PD168393, fully restored the pHe values of IB3-1 cells, suggesting that the reduced pHe is mainly due to the increased EGFR activity and lactate. In addition, in IB3-1 CF cells, the LDHA mRNA, protein expression, and activity are down-regulated under EGFR inhibition. Thus, a constitutive EGFR activation seems to be responsible for the reduced pHe in IB3-1 CF cells.

Keywords: CFTR; cystic fibrosis; EGFR; extracellular pH; IB3-1 cells; lactate; LDH

Introduction

Cystic fibrosis (CF) is an autosomal recessive disease caused by mutations in the cystic fibrosis transmembrane conductance regulator (CFTR) gene (Riordan et al. 1989). CFTR is an ATP-gated chloride (Cl−) channel, activated mainly through PKA phosphorylation (Chin et al. 2017), which also participates directly or indirectly in the transport of bicarbonate (HCO_3^-) (Kunzelmann et al. 2017), glutathione (GSH) (Kogan et al. 2003), and ATP (Egan 2002). Mutations in the CFTR gene affect its expression and functionality leading to the complex CF phenotype (Lim et al. 2017; Riordan 2008; Veit et al. 2016).

Several years ago, we postulated the hypothesis that the complex CFTR phenotype might be the result of a differential gene expression between normal and CF cells (Cafferata et al. 1995). Searching for possible CFTR-dependent genes by using differential display, we found different genes which expression was altered in CF, such as *c-Src* (Gonzalez-Guerrico et al. 2002; Massip-Copiz et al. 2017; Massip Copiz and Santa Coloma 2016), which in turn regulates MUC1 expression (Gonzalez-Guerrico et al. 2002). This was the first signaling effector found for the CFTR signaling pathway. We also found a reduced expression of MTND4, a mitochondrial protein encoded in the mitochondrial DNA, essential for the assembly and activity of the mitochondrial Complex I (Valdivieso et al. 2007; Valdivieso et al. 2012). Thus, we measured the mitochondrial complex I (mCx-I) activity in CF cells and found that its activity was reduced (Clauzure et al. 2014; Valdivieso et al. 2012)(reviewed in (Valdivieso and Santa-Coloma 2013)). Then, we thought that this mCx-I failure could be the reason for the reduced extracellular pH reported in CF cells and tissues (Massip-Copiz and Santa-Coloma 2018), through enhanced aerobic glycolysis. Confirming this hypothesis, we found a decreased pHe, increased LDH activity and lactate secretion in intestinal Caco-2/pRS26 (Caco-2 colon carcinoma cells transfected with an shRNA-CFTR) compared to control Caco-2/pRSCtrl cells, and also in lung IB3-1 CF cells compared to C38 cells (C38 are CFTR “rescue” cells) (Valdivieso et al. 2019).

Interestingly, the inhibition of LDH with oxamate was able to completely revert the pHe differences in Caco-2/pRS26 compared to control Caco-2/pRSCtrl cells, suggesting that, contrary to

what it is generally accepted (reviewed in (Massip-Copiz and Santa-Coloma 2018)), the increased LDH and lactate secretion, and not a reduced bicarbonate secretion, was the preponderant mechanism for the reduced pHe, at least in these colon epithelial cells and also in IB3-1 lung CF cells (Valdivieso et al. 2019). On the other hand, the inhibition of c-Src with PP2 and JNK with SP600125 only partially reverted the pHe differences between CF and control cells, suggesting that some additional signaling events may be involved. In this regard, we found recently that CFTR regulates the expression of EGFR ligands in Caco-2/pRS26 cells (shRNA for CFTR); in particular, epiregulin (EREG) had the strongest response, which is upregulated through an IL-1β autocrine loop (Clauzure et al. 2014; Clauzure et al. 2017; Massip-Copiz et al. 2018; Massip-Copiz et al. 2017). This resulted in an activated EGFR signaling (supplementary figures S1 and S2 in (Massip-Copiz et al. 2018)). Noteworthy, JNK was a downstream effector in the EGFR signaling in these colon carcinoma cells.

Taken into account the activated EGFR signaling observed in CF cells (Burgel et al. 2007; Kim et al. 2013; Martel et al. 2013; Massip-Copiz et al. 2018; Stolarczyk et al. 2018), this work aimed to explore whether or not the EGFR is involved in pHe regulation and LDH expression of IB3-1 CF cells. We used IB3-1 cells since these cells constitutively express IL-1β and EGFR ligands (Massip-Copiz et al. 2018), have an activated EGFR (Massip-Copiz et al. 2018), and a low pHe. We found that the EGFR inhibitors AG1478 (reversible inhibitor) and PD168393 (irreversible inhibitor) lead to an increased pHe in the conditioned media of the IB3-1 CF cells, reaching the pHe values of CFTR “rescued” C38 cells. The effect of these inhibitors on the pHe was due to a decreased lactic acid secretion in the conditioned media. The EGFR inhibitors also diminished the LDH activity and reduced LDHA mRNA and protein expression. These results suggest that EGFR activity plays a key role in regulating LDH expression and activity, lactate production, and secretion. Therefore, the EGFR activity appears to be responsible for the extracellular pH reduction in the conditioned media of IB3-1 CF cells, through lactate (lactic acid) hypersecretion.

MATERIALS AND METHODS

Reagents. L(+)-lactic acid, free acid (Cat. # L1750-10G), protease inhibitor cocktail P2714, and DMSO culture grade were purchased from Sigma-Aldrich (St. Louis, MO). AG1478 was from Calbiochem (San Diego, CA) and PD168393 was from MedChem Express (MCE, Monmouth Junction, NJ). All other reagents were analytical grade. The stock solutions of pathway inhibitors were prepared at 1000 X in culture-grade DMSO. *Antibodies*: anti-rabbit antibody coupled to horseradish peroxidase (polyclonal, W401B) was from Promega (Madison, WI); rabbit polyclonal anti-actin antibody (A2066) was from Sigma-Aldrich, rabbit FITC-conjugated secondary antibody (554020) was from BD Pharmingen, and rabbit monoclonal antibody anti-LDHA (C4B5, Cat. #3582) and rabbit polyclonal antibody anti-phospho-LDHA (Cat. #8176) were from Cell Signaling Technology (Danvers, MA).

Cells. IB3-1 (CRL-2777) and C38 (CRL-2779) cells were purchased from ATCC (www.atcc.org; now available only at John Hopkins University). IB3-1 cells are bronchial epithelial cells derived from a CF patient that had the most frequent mutation, ΔF508, in one allele (Zeitlin et al. 1991). These cells also have the non-sense mutation W1282X in the second allele (Gruenert et al. 2004), which also determines by itself a severe disease (Shoshani et al. 1992). The IB3-1 cells have been immortalized using the hybrid adenovirus adeno-12-SV40 (Zeitlin et al. 1991). C38 cells are IB3-1 cells transduced with an adeno-associated viral vector to stably express a functional CFTR, in a truncated version of CFTR, which retains its Cl^- transport activity (Flotte et al. 1993). All cell lines were cultured in DMEM/F12 with 14.29 mM HCO_3^- and 15.02 mM HEPES (Cat. No. 12500-096, Life Technologies, GIBCO BRL, Rockville, MD) supplemented with 10 % FBS (Internegocios S.A., Mercedes, Buenos Aires, Argentina), 100 U/ml penicillin, 100 µg/ml streptomycin, and 0.25 µg/ml amphotericin B (Life Technologies, GIBCO BRL, Rockville, MD). Cultures were grown in a humidified atmosphere containing 5 % CO_2 at 37 °C.

Measurement of the extracellular pH (pHe)). Cells were cultured in p60 culture dishes (52.8 mm), plated at 6 x 10^4 cells/cm^2 in 3 ml of culture medium (1 x 10^5 cells/dish). After incubation in serum-free medium at the time indicated for each experiment, the pHe was measured in the conditioned

media by using a pH meter (UltraBasic UB-10, Denver Instrument, Bohemia, NY). To avoid pHe changes in the culture medium due to atmospheric equilibration, each plate was maintained in the incubator containing 5 % CO_2 until it was rapidly measured by using the pH meter.

Extracellular lactate measurement. Cells were cultured in p60 culture plates, seeded at a density of 4 x 10^4 cells/cm^2 in 3 ml of culture medium containing 5% FBS. Before treatments, cells were incubated 24 h in 3 ml of serum-free medium to reach basal conditions, and then, the serum-free medium was replaced by a new serum-free medium with or without treatments. After the second incubation in serum-free medium, a sample (15 µl) of the medium was collected at 0, 24, and 48 h, to measure lactate secretion. The samples were centrifuged at 600 x g for 10 min at 4 °C and the lactate concentration was measured in the supernatants by using the Lactate kit from Roche (Cat. # 11822837 190, Roche Diagnostics GmbH, Mannheim, Germany), with some modifications to adapt the measurements to a 96 wells plate spectrophotometer (Multiskan Spectrum, Thermo Fisher Scientific, Vantaa, Finland) (Valdivieso et al. 2019). Briefly, the lactate calibration curve (5, 10, 20, 30, 40, 50, and 100 µM) was made by using a 150 mM lactate stock solution prepared from L(+)-lactic acid dissolved in serum-free DMEM/F12 medium containing 15 mM HEPES and neutralized to pH 7.4 using a 1 M KOH solution. The samples (conditioned media) were diluted 1:100 and 150 µl/well were loaded in 96 wells plates. The lactate kit reagents were mixed, 12.5 µl of R1 (this solution is the hydrogen donor, ascorbate ≥ 30 U/ml, buffer) and 2.5 µl of R2 (4.9 mM 4-aminoantipyrine, lactate oxidase (LOD, microorganisms) ≥ 15 U/ml, horseradish peroxidase ≥ 24 U/ml, buffer) per well, and 15 µl/well were added to the samples and the calibration curve. The spectrophotometric measurement was performed at 660 nm after 5 min of incubation at RT.

Lactate dehydrogenase activity (LDH). Lactate Dehydrogenase Activity was determined spectrophotometrically by measuring the oxidation of NADH during the reduction of pyruvate to lactate (absorbance/min at 340 nm) as previously reported (Chen et al. 1989; Valdivieso et al. 2019).

LDHA reverse transcription and quantitative real-time PCR (qRT-PCR). qRT-PCR assays were performed as previously described (Massip-Copiz et al. 2018; Valdivieso et al. 2012). Briefly, total

RNA was isolated by using a guanidinium thiocyanate-phenol-chloroform extraction solution (Chomczynski and Sacchi 1987, 2006). The quality of RNA was checked by electrophoresis in denaturing formaldehyde agarose gels (Sambrook J 1989), and measuring the ratios A260/A230 (greater than 2) and A260/A280 nm (over 1.7). Reverse transcription (RT) was performed by using 1 μg of total RNA, M-MLV reverse transcriptase (100 U, Promega, Madison, WI), and Oligo-dT12 in a 25 μl final reaction volume, according to manufacturer´s instructions. The reaction was performed for 90 min at 37 ºC, 5 min at 75 ºC, and then cooled to 4 ºC. The synthesized cDNAs were used immediately for PCR amplification or stored at -80 ºC for later use. qRT-PCRs were performed using an ABI 7500 real-time PCR system (Applied Biosystems Inc., Foster City, CA); the ΔΔCt method was used for comparative quantification. TBP (Tata Box Binding Protein) was used as an internal control. The cDNA samples were added to 25 μl of PCR reaction mixture containing a final concentration of 2.5 mM $MgCl_2$, 0.4 mM deoxynucleotide triphosphates, 1 U of Pegasus Taq DNA polymerase, 0.1 X EvaGreen (Biotium, Hayward, CA), 50 nM ROX as a reference dye, and 0.2 nM of each primer. The qRT-PCR conditions were as follows: initial denaturation at 95 ºC for 5 min, followed by 30 cycles at 95 ºC for 30 s, 60 ºC for 30 s, and 72 ºC for 30 s. The fluorescence signal was acquired at the elongation step, at the end of each cycle. qRT-PCR reactions were carried out in triplicates. The final quantification values were expressed as the mean of the Relative Quantification (RQ) for each biological triplicate (n = 3). Primer sequences used in this paper were: LDHA Fwd 5´-ATGGCAACTCTAAAGGATCAGC-3´ Rv 5´- CCAACCCCAACAACT GTAATCT-3´ and TBP Fwd 5´-TGCACAGGAGCCAAGAGTGAA-3´ Rv 5´-CACATCACAG CTCCCCACCA-3´ .

Western Blots. Cells were incubated as above indicated, washed twice with cold PBS, scraped with cold extraction buffer (10 mM Tris pH 7.4, 100 mM NaCl, 0.1% SDS, 0.5% sodium deoxycholate, 1% Triton X-100, 10% glycerol) containing the protease inhibitor cocktail P2714 (5 mL of cocktail/20 g of cell extract) plus phosphatase inhibitors (2 mM Na_3VO_4, 1 mM NaF, and 10 mM Na_2PO_7), and centrifuged at 14 000 x g for 20 min at 4 °C. The supernatant was stored at −80 °C until use. The protein concentration was measured by using the method of Lowry. SDS-PAGE and

Western blots were performed as previously described (Massip-Copiz et al. 2018). The band's intensities were quantified by using the Image J software (http://rsbweb.nih.gov).

Flow cytometry. To obtain more accurate results, LDHA was also quantified by using flow cytometry (Valdivieso et al. 2019). Briefly, IB3-1 cells were cultured as mentioned above, in p60 plates, at 37 °C in a humidified atmosphere containing 5 % CO_2. Cells were harvested with trypsin and washed twice with PBS. Ice-cold samples containing 1 x 10^6 cells per 150 µl of PBS were fixed by adding 50 µl of paraformaldehyde-sucrose 4X (paraformaldehyde 4 %-sucrose 4 % final concentration) to each tube and incubated for 15 min at 4 °C. Cells were washed three times with PBS plus 0.2 % Tween 20 (PBS-T) and centrifuged at 400 x g for 5 min. Unspecific binding sites were blocked with 5% BSA in PBS for 30 min and washed two times with PBS-T and centrifuged at 400 x g for 5 min. Cells were incubated with 50 µl of the anti-LDHA rabbit antibody diluted 1:200 and incubated overnight at 4 °C. Then, cells were washed three times with PBS-T and centrifuged at 400 x g for 5 min. Cells were incubated with 50 µl of the anti-rabbit-FITC antibody diluted 1:400, incubated 1 h at RT, and washed three times with PBS-T. Cells were pelleted by centrifugation at 400 x g for 5 min, resuspended in 300 µl of PBS, and run on the flow cytometer (Accuri, BD Biosciences, San José, CA). To quantify the LDHA content the mean of fluorescence intensity (MFI) was measured and the results were expressed as mean ± SE of three independent experiments, each performed by triplicates.

Confocal immunohistochemistry (IHC). IB3-1 and C38 cells were plated on coverslips in 24-well plates (4×10^4 cells/well; 2×10^4 cells/cm^2) and cultured for 48 h in 2 ml of DMEM-F12 without serum 5%. Immunocytochemistry was performed as previously described (Valdivieso et al. 2019) with some modifications. Briefly, cells were rinsed twice in ice-cold PBS and fixed with a freshly prepared solution of 4% paraformaldehyde in PBS, for 20 min at RT. Then, cells were rinsed 3 times in Tris-Buffered Saline 1× (TBS) and permeabilized with 0.1% Triton X-100 in TBS for 15 min at RT. After three washes in ice-cold TBS, cells were blocked with 5% BSA-TBS for 1 h at room temperature. Then, cells were incubated with a primary anti-LDH-A antibody, dilution 1:200 in 5%

BSA-TBS plus Tween-20 (0.05% v/v) and incubated overnight at 4 ºC. After primary antibody incubation cells were washed three times with TBS plus Tween-20 (0.05% v/v) and incubated with FITC-conjugated secondary antibody, dilution 1:400 in the same buffer for 2 h, at RT. Immunofluorescence images were captured with a Zeiss LSM 510 confocal microscope (Carl Zeiss, Jena, Germany) using a 63X/1.2 NA (NA, numerical aperture) water-immersion objective. For FITC (Ex/Em: 490/525), a 488-laser line was used for excitation and an LP 505 nm filter for emission (green).

Statistics. Unless otherwise indicated, all the results corresponded to the average of three independent experiments (mean ± SD, n=3). One-way ANOVA and Tukey's tests were applied to determine significant differences among samples ($p< 0.05$). In addition, we verified the significant differences using the non-parametric Mann-Whitney or the Kruskal-Wallis (both using medians and CI instead of means and SD). When differences exist in the significance between these tests, they are shown in the figure legends. Significant differences between slopes were calculated by using the online software Free Statistics Calculators (Sopper 2019), using the average slopes and SD values from n = 3 independent experiments (df = 2). The open circles in the graph bars are the average values of each independent experiment.

RESULTS

EGFR activity mediates hyperacidity in the conditioned medium of IB3-1 cells

As shown in Figure 1 A, in agreement with our earlier results, IB3-1 cells have a more acidic pHe compared to C38 cells (IB3-1 pHe = 7.19 ± 0.03; C38 pHe = 7.37 ± 0.04 (n = 3), $p<0.05$ compared to IB3-1 cells). Also, a significant difference was observed in the lactic acid secreted to the extracellular medium of C38 and IB3-1 cells (2.03 ± 0.34 mM vs 4.99 ± 0.32 mM (n = 3), $p<0.05$) incubated in serum-free medium for 48 h (Fig. 1B). As shown in Fig. 1C, there was a time-dependent secretion of lactic acid that increased linearly in both cell lines (0, 24, and 48 h). The rate for lactate production was significantly ($p < 0.05$, df = 2, t = 4.62) higher in IB3-1 cells (slope = 0.084 ± 0.009

(n=3), $R^2 = 0.99$) than in C38 cells (slope = 0.026 ± 0.006 (n=3), $R^2 = 0.95$). In agreement with these results, the intracellular LDH activity (Fig. 1D) showed a significant rise ($p < 0.05$) in IB3-1 cells (154 % ± 13.0 %, n = 3) compared to control cells (100 % ± 3.2, n = 3).

To determine whether the EGFR receptor was involved in pHe regulation, IB3-1 and C38 cells were incubated 24 h in serum-free media, and then treated with the EGFR inhibitors AG1478 (tyrphostin AG-1478) and PD168393, for 48 h. These inhibitors were chosen since they are potent, specific, and have different mechanisms of action, decreasing the probability of simultaneous nonspecific off-target effects. AG1478 is a potent and reversible EGFR kinase inhibitor that blocks EGFR tyrosine kinase activity and autophosphorylation (Levitzki and Gazit 1995; Osherov and Levitzki 1994); it also induces the formation of inactive, unphosphorylated EGFR dimers in the presence or absence of the ligand (Arteaga et al. 1997). AG-1478 has an IC_{50} *in vitro* of 3 nM (Levitzki and Gazit 1995) and an EC_{50} of 34.6 µM in cultured U87MG cells (MG stands for malignant glioma) (Han et al. 1996). At 20 µM, AG1478 inhibits EGFR phosphorylation at Tyr1173 in MDA-MB-231 breast cancer cells (D'Anneo et al. 2013). AG1478 inhibited EGF-stimulated mitogenesis without affecting PDGF-induced DNA synthesis and [3H]-Thymidine uptake stimulated by FGF-2 was not affected by AG1478 at 100 µM (Rice et al. 1999). The ED50 against HER2-Neu and PDGFR is over 100 µM (Levitzki and Gazit 1995).

On the other hand, PD168393 is a potent, irreversible kinase inhibitor of EGFR and ErbB2 that alkylate Cys-773 by docking into the ATP binding pocket of EGFR tyrosine kinase, in the cytoplasmic side of the receptor; it showed an IC_{50} of 0.7 nM (purified EGFR kinase) and EC50 of 1.3 nM in HS-27 human fibroblasts, and an EC_{50} of 4.3 nM in A431 cells, for EGF-induced (100 ng/ml EGF, 5 min) EGFR autophosphorylation (2 µM during 1 h preincubation to reach 100 irreversible inhibition) (Fry et al. 1998). it is inactive against insulin, platelet-derived growth factor, and basic FGF receptor TKs, as well as protein kinase C at 50 µM (Fry et al. 1998).

To make sure that we were using the adequate concentrations of inhibitors, dose-response curves were obtained (Fig. 2A and Fig. 2B). IB3-1 cells were treated with increased concentrations

of AG1478 or PD168393 and the pHe was measured in conditioned media after 48 h incubation. As shown in Figure 2A, AG1478 showed an EC_{50} = 5.9 ± 0.3 (n=3) μM, with a plateau starting at 10 μM, which is the concentration used by Takai et al. with several ovarian cell lines (Takai et al. 2010). On the other hand, as shown in Figure 2B, the inhibitor PD168393 showed an EC_{50} = 2.1 ± 0.5 (n=3) μM, with a plateau at 10 μM, which is the concentration previously used by Sun et al. in mouse cardiomyocytes (Sun et al. 2015). The different mechanisms of action of these inhibitors decrease the probability of similar off-target effects. Nevertheless, off-target effects have been observed in other model systems for both inhibitors (Douglas et al. 2009; Shi et al. 2009). Also, other members of the EGFR family, such as erbB2, could be involved in the observed effects; therefore, these results should be taken with caution. We performed dose-response curves to determine the adequate doses for these inhibitors that affect the pHe of IB3-1 cells. We selected a 10 μM concentration since this concentration already showed a plateau. This concentration of AG1478 was already used with IB3-1 and C38 cells by Kim et al., showing these authors that 10 μM inhibited the EGFR phosphorylation at Y1068 in both IB3-1 and C38 cells (Kim et al. 2013). Thus, both inhibitors were then used at 10 μM, which is considered a still acceptable concentration to avoid off-target effects (Knight and Shokat 2005).

As shown in Figure 2C, there was a significant ($p < 0.05$) decrease in the pHe of IB3-1 cells (7.19 ± 0.03, n = 3) compared to the pHe of CF corrected cells C38 (7.37 ± 0.04, n=3), which is a value within the physiological range of 7.35-7.45 for blood; below 7.35 is considered acidemia (Hopkins et al. 2020). When the cells were cultured in the presence of the EGFR inhibitor AG1478 (10 μM, 48 h) there was a significant increment in the pHe compared with untreated control cells (7.36 ± 0.01 vs 7.19 ± 0.03, n = 3, $p<0.05$). AG1478 slightly increased the pHe of C38 cells, although the values did not reach a significant difference. Similarly, as shown in Figure 2D, IB3-1 cells treated with the irreversible EGFR inhibitor PD168393 (10 μM, 48 h) also increased their pHe (7.19 ± 0.03 vs 7.35 ± 0.02, n = 3). However, as shown in Figure 2D, in contrast to AG1478, PD168393 did not have any observable effect on C38 cells, and the pHe recovery was almost complete with this

inhibitor (7.35 ± 0.03, n=3), compared to C38 cells (7.37 ± 0.04, n=3). This full recovery in the pHe suggests that the observed pHe reduction in IB3-1 cells is entirely due to EGFR activation.

EGFR modulates LDH activity and lactic acid production

Considering the effect of the EGFR in the pHe regulation shown above, we thought to determine whether EGFR also regulates lactic acid secretion (measured as lactate) and LDH activity. These parameters were measured in IB3-1 and C38 cells treated with the EGFR inhibitors AG1478 and PD168393. Fig 3A shows a decreased LDH activity in IB3-1 cells treated with AG1478 compared with control cells (154 ± 13 % vs. 120 ± 4.9 %, n = 3, $p < 0.05$). In the same way, as shown in Fig. 3B, IB3-1 cells treated with PD168393 also decreased their LDH activity (154 ± 9.7 % vs 85 ± 5.1 %, n = 3, $p < 0.05$). Both inhibitors had no effects on the LDH activity of C38 cells. Regarding lactate, as shown in Fig. 3C and 3D, after 48 h, these inhibitors also significantly ($p < 0.05$) decreased the lactate secretion in IB3-1 cells. There is a time-dependent secretion of lactate that increased linearly in IB3-1 cells with or without inhibitors; however, the rate for lactate production was significantly ($p< 0.05$) lower in IB3-1 cells treated with AG1478 (slope = 0.066 ± 0.010, n=3) (Fig. 3C) or PD168393 (slope = 0.048 ± 0.011, n=3) (Fig. 3D) than in IB3-1 cells without treatment (slope = 0.084 ± 0.009, n=3). The effects on IB3-1 CF cells were stronger with the irreversible inhibitor PD168393. However, although these inhibitors fully restored the pHe, only partially restored the lactate levels compared to C38 cells after 48 h incubation (IB3-1 4.99 ± 0.32 mM (n = 3), n=3; IB3-1 AG1478 3.68 ± 0.60 mM, n=3; IB3-1 PD168393 3.60 ± 0.75 mM, n=3; vs. C38 2.03 ± 0.24 mM; n=3). There was always a basal lactate production independent of the EGFR activity.

LDHA expression is upregulated in IB3-1 cells

Then, we want to determine if the increased LDH activity and lactic acid secretion correlated with LDHA expression in IB3-1 cells. We observed a significantly increased mRNA expression of

LDHA (Fig. 4A) in IB3-1 cells compared to C38 cells (163 ± 18.5 % vs. 100 ± 5 %, n=3). When we analyzed the protein expression by Western blots (Fig. 4B), there was also an increased expression, not only in total LDHA (100 ± 4.4 % vs. 146 ± 9.7 %, n=3) (Fig. 4C) but also in p-Tyr10-LDHA (100 ± 4.5 % vs. 135 ± 10 %, n=3) (Fig. 4D). The expression of LDHA was also analyzed by confocal microscopy. As shown in Figure E, IB3-1 cells showed an increased green FITC fluorescence signal corresponding to the secondary Ab against anti-LDHA, compared to C38 cells. The differences in LDHA expression observed by WBs and confocal microscopy were then quantified by using flow cytometry, which provides a more reliable quantification, cell by cell (Fig. 4F-I). LDHA and p-LDHA expression levels were expressed as Mean Fluorescence Intensity (MFI). The LDHA expression (100 ± 7 % vs. 160 ± 38 %, n=3) (Fig. 4F, 4G) and the p- Tyr10-LDHA expression (100 ± 1 % vs. 195 ± 9 %, n=3) (Fig. 4H, 4I) were both significantly higher ($p<0.05$, n=3) in IB3-1 cells than in C38 cells. The increased p-Tyr10-LDHA suggests that LDHA was not only overexpressed in IB3-1 cells but also activated through tyrosine phosphorylation. However, the ratio p-Tyr10-LDHA/LDHA remained approximately constant (the differences in the ratios were not significant; results not shown), suggesting that the overexpressed LDHA is activated in the same proportion. The kinase(s) responsible remains to be determined. These results suggest that LDHA and p-LDHA are up-regulated in CF cells, in agreement with the observed increase in LDH activity and lactate secretion.

EGFR modulates LDHA expression

Since *LDHA* expression (mRNA and protein) and activity increased in CF IB3-1 cells, we wanted to know whether LDHA expression was also affected by the EGFR activity. To test this, IB3-1 and C38 cells were incubated in the presence of the EGFR inhibitors and the LDHA mRNA expression levels were measured by quantitative real-time PCR. As shown in Figure 5A, the EGFR inhibitors significantly reduced the LDHA mRNA expression (IB3-1 100 ± 10 %, AG1478 52.9 ± 7.4 %, PD168393 65.3 ± 1.8 %, n=3). This was confirmed by flow cytometry, analyzing the expression of total LDHA (Fig. 5B and 5C). LDHA protein expression levels were expressed as

Mean Fluorescence Intensity (MFI) (Fig. 5B). Representative cytometries are shown in Figure 5C, plotted as FL1-A (Fluorescence intensity of green channel or FL1-A) vs FSC-A (forward scattering). The results showed a significantly ($p<0.05$, n=3) decreased LDHA expression in IB3-1 cells treated with the EGFR inhibitors AG1478 and PD 168393 (IB3-1 100 ± 10 %, AG1478 60 ± 18 %, PD168393 80 ± 8 %, n=3). Therefore, EGFR activity also regulates LDHA mRNA and protein expression.

DISCUSSION

As a model system we used cultured IB3-1 airway CF cells, which have a mutated CFTR (ΔF508/W1282X genotype), and C38 cells, which are IB3-1 "corrected cells", transduced with a viral vector expressing a truncated wt-CFTR, which resulted in a high basal CFTR activity (Flotte et al. 1993). We used IB3-1 CF cells, cultured as nonconfluent monolayers since these cells, with impaired CFTR activity, have a constitutive secretion of IL-1β (Clauzure et al. 2014; Clauzure et al. 2017; Massip-Copiz et al. 2017), which in Caco-2/pRS26 cells activates the expression of EGF ligands through JNK (but not c-Src) and keeps an activated EGFR signaling (Massip-Copiz et al. 2018), and inflammatory state (Yang et al. 2019). Thus, with IB3-1 cells there is not a need to add external stimuli that can produce unnecessary off-target effects and complicate the interpretation of the results. Also to avoid off-target effects of the dibutyryl-cAMP, isoproterenol, and the IBMX (3-isobutyl-1-methylxanthine) used for CFTR stimulation, we decided to perform the cultures in the absence of CFTR stimulation and use C38 (des-1-119-CFTR) cells instead of S9 (IB3-1 cells expressing wt-CFTR) cells. We did not use S9 cells since these cells need CFTR stimulation to show differences in activity compared to IB3-1 cells. On the other hand, C38 cells, without stimulation, already have increased rates of Cl^- efflux compared to IB3-1 cells (Flotte et al. 1993), and do not necessarily need stimulation to show differences with IB3-1 cells. CFTR is overexpressed in C38 cells compared to IB3-1 cells (Andersson et al. 2008), and this might explain the increased basal CFTR activity in C38 cells. When the activity of the mitochondrial Complex I (mCx-I) was measured; differences between S9 and IB3-1 cells were observed only upon stimulation (Valdivieso et al. 2012). Also, S9 cells need CFTR stimulation to show differences with IB3-1 cells in IL-1β

secretion (Clauzure et al. 2017). When the intracellular chloride was measured in S9 and IB3-1 cells, it became evident that in the presence of a stimulation cocktail (200 mM dibutyryl cAMP, 200 mM IBMX, and 20 mM isoproterenol), the IB3-1 cells have some residual CFTR activity, as occurs in CF patients (Sermet-Gaudelus et al. 2002); the chloride increases in the presence of CFTR(inh)-172, and S9 cells have less intracellular chloride than IB3-1 cells because the CFTR is functional (Clauzure et al. 2017). This was also reflected in the secretion of lactate by IB3-1 cells compared with C38 cells(Valdivieso et al. 2019).

In previous studies, IL-1β strongly acidified the conditioned media of Caco-2/pRSctrl cells and mediated the increased NOX1/4 and ROS levels and decreased pHe, in Caco-2/pRSctrl and IB3-1 cells, through an autocrine positive feedback signaling, in which c-Src and JNK were involved (Clauzure et al. 2014; Clauzure et al. 2017; Massip-Copiz et al. 2017; Valdivieso et al. 2019). Also, the IL-1β autocrine loop induced EGFR ligands, particularly epiregulin. This resulted in an activated p-EGFR in cells with impaired CFTR activity (Massip-Copiz et al. 2018). Then, we noted that besides epiregulin (EREG) upregulation, c-Src and JNK may be downstream singling effectors for EGFR, opening the possibility that the observed IL-1β effects on pHe were indirectly mediated by EGFR signaling. Thus, using two pharmacological inhibitors of EGFR that act through different mechanisms (one reversible and the other irreversible) we assessed this hypothesis.

In the present work, we first measured the pHe, lactate levels, and LDH expression and activity in IB3-1 CF cells and C38. The results showed that a reduced pHe is present in the conditioned media of IB3-1 cells compared to the pHe values of the CFTR-corrected C38 cells (Fig. 1), confirming our previous observations (Valdivieso et al. 2019). The LDHA was found overexpressed in IB3-1 cells, as determined by WBs, confocal microscopy, and flow cytometry. The cytometric results (fluorescence measured in each of 10.000 cells) suggests that the reduction in the pHe and hypersecretion of lactate in IB3-1 cells should not only be attributed to possible accelerated growth of IB3-1 cells compared to C38 cells but rather to an increased LDH expression in each cell. The cells accumulated a large amount of lactate, reaching a concentration near 5 mM after 48 h. This represents a huge amount of lactate, but still far from the buffering capacity of the DMEM-F12

391 medium with 15 mM HEPES and 15 mM bicarbonate. A key question is, therefore, which is the
392 buffer capacity of the ASL and the basolateral compartment. Only when the buffer capacity is
393 exceeded, we will see a drastic reduction in the pHe. This might explain some of the contradictory
394 results regarding the pHe in CF cells. Also, to measure lactate is a better measure than pHe, since
395 only when the buffer capacity is exceeded a drastic reduction on the pHe will be noted.

396 Incubation of IB3-1 CF cells with the reversible EGFR inhibitor AG1478 partially restored
397 the pHe levels of IB3-1 cells compared to the values of C38 control cells (C38 are IB3-1 CF cells
398 expressing wt-CFTR). AG1478 restore the IB3-1 cells to the values of untreated C38 cells, but basal
399 values of C38 cells were also increased by AG1478. On the contrary, the irreversible (alkylating)
400 EGFR inhibitor PD168393 did not affect basal values of C38 cells and fully restored the pHe of IB3-
401 1 cells compared to C38 cells. Furthermore, these EGFR inhibitors decreased LDHA expression,
402 LDH activity, and lactate production. These effects are in agreement with the results reported by
403 Coaxum et al. (Coaxum et al. 2009) in cultured renal glomerular podocytes stimulated with EGF, in
404 which the EGFR tyrosine kinase inhibitor AG1478 inhibited the extracellular acidification rate
405 (ECAR), although the ECAR effect was attributed to the EGF activation of Na^+/H^+ exchange. One
406 may think that at least partially the Na^+/H^+ exchanger may contribute to the decreased pHe in IB3-1
407 cells. However, our previous results with IB3-1 and C38 cells (Valdivieso et al. 2019) showed an
408 almost complete recovery of the pHe of IB3-1 cells, compared to C38 cells, by incubation with the
409 LDH inhibitor oxamate.

410 Our results regarding EGFR upregulation in IB3-1 cells are in agreement with previous
411 results obtained in CF bronchial epithelial CFBE41o(-) cells lacking functional CFTR cultured at the
412 air-liquid interface (ALI). This was confirmed by using differentiated primary human bronchial
413 epithelial cells (HBEC-ALI) (Stolarczyk and Scholte 2018; Stolarczyk et al. 2018). An activated
414 EGFR signaling pathway was also observed by Martel et al. (Martel et al. 2013) in CFTR ΔF508-
415 expressing airway epithelial cells exposed to Pseudomonas aeruginosa. On the other hand, our results
416 regarding the differences in LDHA expression levels between IB3-1 and C38 cells are in agreement

with a recent proteomic analysis of these cells (Ciavardelli et al. 2013); this LDHA upregulation has been also observed in the bronchial and nasal epithelium from CF patients (Ogilvie et al. 2011; Polineni et al. 2018). LDH shows a complex regulation and several transcription factors and kinases regulates its activity (Mishra and Banerjee 2019). Increased expression of EGFR has been reported by Burgel et al. in patients with cystic fibrosis (Burgel et al. 2007). Also, Martel et al. (Martel et al. 2013) observed an increased EGFR phosphorylation (at Tyr-1068) in the CF airway epithelium and sub-epithelial inflammatory cells of CF lung biopsies (Martel et al. 2013). Furthermore, it was reported that p-EGFR is increased in IB3-1 cells (CF) compared to C38 cells (Kim et al. 2013), and recently, this was also observed in the human CF bronchial epithelial cell line CFBE41o- (Stolarczyk et al. 2018) and in Caco-2/pRS26 cells (Fig. S1 in Massip-Copiz et al.(Massip-Copiz et al. 2018)).

Taken together, these results suggest that the EGFR receptor has a key role in regulating LDHA expression and activity in IB3-1 CF cells, which in turn determines an increased acid lactic secretion and decreased pHe. Taken into account our recent results with IB3-1 and Caco-2 cells (Clauzure et al. 2014; Clauzure et al. 2017; Massip-Copiz et al. 2018; Massip-Copiz et al. 2017; Valdivieso and Santa-Coloma 2019; Valdivieso et al. 2016; Valdivieso et al. 2019), it appears that the mechanisms of hyperacidity in cells with impaired CFTR activity involve the CFTR→ Cl^-→ IL-1β,c-Src→ EREG→ EGFR→ c-Src, JNK → LDHA→ lactate axis. We added here the role of EGFR in this mechanism, which is crucial since its inhibition completely restores the pHe to the values of control C38 cells, a physiological value of pHe=7.37. Noteworthy, the more specific and irreversible EGFR inhibitor PD168393 had a zero influence on the pHe of C38 cells, reinforcing the important role of EGFR signaling in the reduced pHe observed here in IB3-1 cells and previously in Caco-2/pRS26 cells. The relationships between the different signaling pathways studied here are illustrated in Figure 6 as a working hypothesis that summarizes and helps to understand the results obtained.

In conclusion, these results suggest that extracellular acidification of CF epithelial cells IB3-1 is partially mediated by the activation of the EGFR signaling, which results in the upregulation of

LDH-A (mRNA and protein), increased LDH activity, and lactate secretion. The EGFR downstream signaling involved in LDHA expression and activity, besides the previously found c-Src and JNK (Valdivieso et al. 2019), is still to be determined. Increased intracellular and extracellular lactate concentrations might have a strong physiological (Latham et al. 2012) and pathophysiological (Feng et al. 2018; Lardner 2001; Martinez et al. 2007; Massip-Copiz and Santa-Coloma 2018) consequences in cells in which the EGFR signaling is activated through the CFTR failure or in conditions using a different mechanism to activate EGFR, such as those occurring in cancer. These results indicate that EGFR signaling is a new effector in the CFTR and Cl^- signaling pathways.

ACKNOWLEDGMENTS

We thank Diego Battiato and Romina D'Agostino for administrative assistance. This work was supported by The National Scientific and Technical Research Council of Argentina (CONICET) [grants numbers: PIP 2015-2017 11220150100227CO and PUE 2016 22920160100129CO to TASC], the National Agency for the Promotion of Science and Technology (ANPCYT) [grant number PICT-2018 04429 to TASC], and The Pontifical Catholic University of Argentina (UCA) to TASC. Fellowships from CONICET to MMMC, CM, and MC and The Pontifical Catholic University of Argentina (UCA) to MMMC.

REFERENCES

Alka, K., and Casey, J.R. 2014. Bicarbonate transport in health and disease. IUBMB Life **66**(9): 596-615. doi:10.1002/iub.1315.

Andersson, C., Al-Turkmani, M.R., Savaille, J.E., Alturkmani, R., Katrangi, W., Cluette-Brown, J.E., et al. 2008. Cell culture models demonstrate that CFTR dysfunction leads to defective fatty acid composition and metabolism. J. Lipid Res. **49**(8): 1692-1700. doi:10.1194/jlr.M700388-JLR200.

Arteaga, C.L., Ramsey, T.T., Shawver, L.K., and Guyer, C.A. 1997. Unliganded epidermal growth factor receptor dimerization induced by direct interaction of quinazolines with the ATP binding site. J. Biol. Chem. **272**(37): 23247-23254. doi:10.1074/jbc.272.37.23247.

Bardon, A. 1987. Cystic fibrosis. Carbohydrate metabolism in CF and in animal models for CF. Acta Paediatr. Scand. Suppl. **332**: 1-30.

Bardon, A., Ceder, O., and Kollberg, H. 1986. Increased activity of four glycolytic enzymes in cultured fibroblasts from cystic fibrosis patients. Res. Commun. Chem. Pathol. Pharmacol. **51**(3): 405-408.

Benedetto, R., Centeio, R., Ousingsawat, J., Schreiber, R., Janda, M., and Kunzelmann, K. 2020. Transport properties in CFTR-/- knockout piglets suggest normal airway surface liquid pH and enhanced amiloride-sensitive Na(+) absorption. Pflugers Arch. **472**(10): 1507-1519. doi:10.1007/s00424-020-02440-y.

Borowitz, D. 2015. CFTR, bicarbonate, and the pathophysiology of cystic fibrosis. Pediatr. Pulmonol. **50 Suppl 40**: S24-S30. doi:10.1002/ppul.23247.

Brouillard, F., Bouthier, M., Leclerc, T., Clement, A., Baudouin-Legros, M., and Edelman, A. 2001. NF-kappa B mediates up-regulation of CFTR gene expression in Calu-3 cells by interleukin-1beta. J. Biol. Chem. **276**(12): 9486-9491. doi:10.1074/jbc.M006636200.

Burgel, P.R., Montani, D., Danel, C., Dusser, D.J., and Nadel, J.A. 2007. A morphometric study of mucins and small airway plugging in cystic fibrosis. Thorax **62**(2): 153-161. doi:10.1136/thx.2006.062190.

Cafferata, E.G., González-Guerrico, A., Pivetta, O.H., and Santa-Coloma, T.A. 1995. Abstract M99 [Identificación mediante “differential display” de genes específicamente regulados por diferentes factores que afectan la expresión del CFTR (canal de cloro afectado en Fibrosis Quística)] Abstracts of the 31th Annual Meeting of the Argentine Society for Biochemistry and Molecular Biology Research, 15-18 November, Villa Giardino, Córdoba, Argentina. Abstracs Book.

Cafferata, E.G., Guerrico, A.M., Pivetta, O.H., and Santa-Coloma, T.A. 2001. NF-kappaB activation is involved in regulation of cystic fibrosis transmembrane conductance regulator (CFTR) by interleukin-1beta. J. Biol. Chem. **276**(18): 15441-15444. doi:10.1074/jbc.M010061200.

Cafferata, E.G., Gonzalez-Guerrico, A.M., Giordano, L., Pivetta, O.H., and Santa-Coloma, T.A. 2000. Interleukin-1beta regulates CFTR expression in human intestinal T84 cells. Biochim. Biophys. Acta **1500**(2): 241-248. doi:10.1016/S0925-4439(99)00105-2.

Ciavardelli, D., D'Orazio, M., Pieroni, L., Consalvo, A., Rossi, C., Sacchetta, P., et al. 2013. Proteomic and ionomic profiling reveals significant alterations of protein expression and calcium homeostasis in cystic fibrosis cells. Mol. Biosyst. **9**(6): 1117-1126. doi:10.1039/c3mb25594h.

Clauzure, M., Valdivieso, A.G., Massip Copiz, M.M., Schulman, G., Teiber, M.L., and Santa-Coloma, T.A. 2014. Disruption of interleukin-1beta autocrine signaling rescues complex I activity and improves ROS levels in immortalized epithelial cells with impaired cystic fibrosis transmembrane conductance regulator (CFTR) function. PLoS One **9**(6): e99257. doi:10.1371/journal.pone.0099257.

Clauzure, M., Valdivieso, A.G., Massip-Copiz, M.M., Mori, C., Dugour, A.V., Figueroa, J.M., et al. 2017. Intracellular Chloride Concentration Changes Modulate IL-1beta Expression and Secretion in Human Bronchial Epithelial Cultured Cells. J. Cell. Biochem. **118**(8): 2131-2140. doi:10.1002/jcb.25850.

Coakley, R.D., and Boucher, R.C. 2001. Regulation and functional significance of airway surface liquid pH. JOp **2**(4 Suppl): 294-300.

Coakley, R.D., Grubb, B.R., Paradiso, A.M., Gatzy, J.T., Johnson, L.G., Kreda, S.M., et al. 2003. Abnormal surface liquid pH regulation by cultured cystic fibrosis bronchial epithelium. Proc. Natl. Acad. Sci. U. S. A. **100**(26): 16083-16088. doi:10.1073/pnas.2634339100.

Coaxum, S.D., Garnovskaya, M.N., Gooz, M., Baldys, A., and Raymond, J.R. 2009. Epidermal growth factor activates Na(+/)H(+) exchanger in podocytes through a mechanism that involves Janus kinase and calmodulin. Biochim. Biophys. Acta **1793**(7): 1174-1181. doi:10.1016/j.bbamcr.2009.03.006.

Chen, E.P., Soderberg, P.G., MacKerell, A.D., Jr., Lindstrom, B., and Tengroth, B.M. 1989. Inactivation of lactate dehydrogenase by UV radiation in the 300 nm wavelength region. Radiat. Environ. Biophys. **28**(3): 185-191. doi:10.1007/bf01211255.

Chin, S., Hung, M., and Bear, C.E. 2017. Current insights into the role of PKA phosphorylation in CFTR channel activity and the pharmacological rescue of cystic fibrosis disease-causing mutants. Cell. Mol. Life Sci. **74**(1): 57-66. doi:10.1007/s00018-016-2388-6.

Chomczynski, P., and Sacchi, N. 1987. Single-step method of RNA isolation by acid guanidinium thiocyanate-phenol-chloroform extraction. Anal. Biochem. **162**(1): 156-159. doi:10.1006/abio.1987.9999.

Chomczynski, P., and Sacchi, N. 2006. The single-step method of RNA isolation by acid guanidinium thiocyanate-phenol-chloroform extraction: twenty-something years on. Nat. Protoc. **1**(2): 581-585. doi:10.1038/nprot.2006.83.

D'Anneo, A., Carlisi, D., Emanuele, S., Buttitta, G., Di Fiore, R., Vento, R., et al. 2013. Parthenolide induces superoxide anion production by stimulating EGF receptor in MDA-MB-231 breast cancer cells. Int. J. Oncol. **43**(6): 1895-1900. doi:10.3892/ijo.2013.2137.

Douglas, M.R., Morrison, K.C., Jacques, S.J., Leadbeater, W.E., Gonzalez, A.M., Berry, M., et al. 2009. Off-target effects of epidermal growth factor receptor antagonists mediate retinal ganglion cell disinhibited axon growth. Brain **132**(Pt 11): 3102-3121. doi:10.1093/brain/awp240.

Egan, M.E. 2002. CFTR-associated ATP transport and release. Methods Mol. Med. **70**: 395-406. doi:10.1385/1-59259-187-6:395.

Eichenlaub, T., Villadsen, R., Freitas, F.C.P., Andrejeva, D., Aldana, B.I., Nguyen, H.T., et al. 2018. Warburg Effect Metabolism Drives Neoplasia in a Drosophila Genetic Model of Epithelial Cancer. Curr. Biol. **28**(20): e6. doi:10.1016/j.cub.2018.08.035.

Erra Díaz, F., Dantas, E., and Geffner, J. 2018. Unravelling the Interplay between Extracellular Acidosis and Immune Cells. Mediators Inflamm. **2018**: 1218297. doi:10.1155/2018/1218297.

Favia, M., de Bari, L., Lassandro, R., and Atlante, A. 2019. Modulation of glucose-related metabolic pathways controls glucose level in airway surface liquid and fight oxidative stress in cystic fibrosis cells. J. Bioenerg. Biomembr. **51**(3): 203-218. doi:10.1007/s10863-019-09797-5.

Feng, Y., Xiong, Y., Qiao, T., Li, X., Jia, L., and Han, Y. 2018. Lactate dehydrogenase A: A key player in carcinogenesis and potential target in cancer therapy. Cancer Med **7**(12): 6124-6136. doi:10.1002/cam4.1820.

579 Flotte, T.R., Afione, S.A., Solow, R., Drumm, M.L., Markakis, D., Guggino, W.B., et al. 1993.
580 Expression of the cystic fibrosis transmembrane conductance regulator from a novel adeno-
581 associated virus promoter. J. Biol. Chem. **268**(5): 3781-3790.
582
583 Fry, D.W., Bridges, A.J., Denny, W.A., Doherty, A., Greis, K.D., Hicks, J.L., et al. 1998. Specific,
584 irreversible inactivation of the epidermal growth factor receptor and erbB2, by a new class of
585 tyrosine kinase inhibitor. Proc. Natl. Acad. Sci. U. S. A. **95**(20): 12022-12027.
586 doi:10.1073/pnas.95.20.12022.
587
588 Garnett, J.P., Hickman, E., Burrows, R., Hegyi, P., Tiszlavicz, L., Cuthbert, A.W., et al. 2011. Novel
589 role for pendrin in orchestrating bicarbonate secretion in cystic fibrosis transmembrane
590 conductance regulator (CFTR)-expressing airway serous cells. J. Biol. Chem. **286**(47): 41069-
591 41082. doi:10.1074/jbc.M111.266734.
592
593 Garnett, J.P., Kalsi, K.K., Sobotta, M., Bearham, J., Carr, G., Powell, J., et al. 2016. Hyperglycaemia
594 and Pseudomonas aeruginosa acidify cystic fibrosis airway surface liquid by elevating epithelial
595 monocarboxylate transporter 2 dependent lactate-H(+) secretion. Sci. Rep. **6**: 37955.
596 doi:10.1038/srep37955.
597
598 Gonzalez-Guerrico, A.M., Cafferata, E.G., Radrizzani, M., Marcucci, F., Gruenert, D., Pivetta, O.H.,
599 et al. 2002. Tyrosine kinase c-Src constitutes a bridge between cystic fibrosis transmembrane
600 regulator channel failure and MUC1 overexpression in cystic fibrosis. J. Biol. Chem. **277**(19):
601 17239-17247. doi:10.1074/jbc.M112456200.
602
603 Gruenert, D.C., Willems, M., Cassiman, J.J., and Frizzell, R.A. 2004. Established cell lines used in
604 cystic fibrosis research. Journal of Cystic Fibrosis **3**: 191-196. doi:10.1016/j.jcf.2004.05.040.
605

606 Han, Y., Caday, C.G., Nanda, A., Cavenee, W.K., and Huang, H.J. 1996. Tyrphostin AG 1478
607 preferentially inhibits human glioma cells expressing truncated rather than wild-type epidermal
608 growth factor receptors. Cancer Res. **56**(17): 3859-3861.
609
610 Hopkins, E., Sanvictores, T., and Sharma, S. 2020. Physiology, acid base balance. StatPearls
611 Publishing; 2020 Jan-. Available from: https://www.ncbi.nlm.nih.gov/books/NBK507807/.
612
613 Huang, J., Kim, D., Shan, J., Abu-Arish, A., Luo, Y., and Hanrahan, J.W. 2018. Most bicarbonate
614 secretion by Calu-3 cells is mediated by CFTR and independent of pendrin. Physiol Rep **6**(5):
615 e13641. doi:10.14814/phy2.13641.
616
617 Jancic, C.C., Cabrini, M., Gabelloni, M.L., Rodríguez Rodrigues, C., Salamone, G., Trevani, A.S.,
618 et al. 2012. Low extracellular pH stimulates the production of IL-1β by human monocytes.
619 Cytokine **57**(2): 258-268. doi:10.1016/j.cyto.2011.11.013.
620
621 Kim, S., Beyer, B.A., Lewis, C., and Nadel, J.A. 2013. Normal CFTR inhibits epidermal growth
622 factor receptor-dependent pro-inflammatory chemokine production in human airway epithelial
623 cells. PLoS One **8**(8): e72981. doi:10.1371/journal.pone.0072981.
624
625 Knight, Z.A., and Shokat, K.M. 2005. Features of selective kinase inhibitors. Chem. Biol. **12**(6):
626 621-637. doi:10.1016/j.chembiol.2005.04.011.
627
628 Kogan, I., Ramjeesingh, M., Li, C., Kidd, J.F., Wang, Y., Leslie, E.M., et al. 2003. CFTR directly
629 mediates nucleotide-regulated glutathione flux. EMBO J. **22**(9): 1981-1989.
630 doi:10.1093/emboj/cdg194.
631

632 Kottmann, R., Phipps, R., and Sime, P. 2013. Reply: from idiopathic pulmonary fibrosis to cystic
633 fibrosis: got lactate? Am. J. Respir. Crit. Care Med. **188**(1): 111-112. doi:10.1164/rccm.201301-
634 0145LE.
635
636 Kottmann, R.M., Kulkarni, A.A., Smolnycki, K.A., Lyda, E., Dahanayake, T., Salibi, R., et al. 2012.
637 Lactic acid is elevated in idiopathic pulmonary fibrosis and induces myofibroblast differentiation
638 via pH-dependent activation of transforming growth factor-β. Am. J. Respir. Crit. Care Med.
639 **186**(8): 740-751. doi:10.1164/rccm.201201-0084OC.
640
641 Kraus, S., Benard, O., Naor, Z., and Seger, R. 2003. c-Src is activated by the epidermal growth factor
642 receptor in a pathway that mediates JNK and ERK activation by gonadotropin-releasing hormone
643 in COS7 cells. J. Biol. Chem. **278**(35): 32618-32630. doi:10.1074/jbc.M303886200.
644
645 Kunzelmann, K., Schreiber, R., and Hadorn, H.B. 2017. Bicarbonate in cystic fibrosis. J Cyst Fibros
646 **16**(6): 653-662. doi:10.1016/j.jcf.2017.06.005.
647
648 Lardner, A. 2001. The effects of extracellular pH on immune function. J. Leukoc. Biol. **69**(4): 522-
649 530. doi:10.1189/jlb.69.4.522.
650
651 Latham, T., Mackay, L., Sproul, D., Karim, M., Culley, J., Harrison, D.J., et al. 2012. Lactate, a
652 product of glycolytic metabolism, inhibits histone deacetylase activity and promotes changes in
653 gene expression. Nucleic Acids Res. **40**(11): 4794-4803. doi:10.1093/nar/gks066.
654
655 Levitzki, A., and Gazit, A. 1995. Tyrosine kinase inhibition: an approach to drug development.
656 Science **267**(5205): 1782-1788. doi:10.1126/science.7892601.
657

Lim, S.H., Legere, E.A., Snider, J., and Stagljar, I. 2017. Recent Progress in CFTR Interactome Mapping and Its Importance for Cystic Fibrosis. Front. Pharmacol. **8**: 997. doi:10.3389/fphar.2017.00997.

Luckie, D.B., Singh, C.N., Wine, J.J., and Wilterding, J.H. 2001. CFTR activation raises extracellular pH of NIH/3T3 mouse fibroblasts and C127 epithelial cells. J. Membr. Biol. **179**(3): 275-284. doi:10.1007/s002320010052.

Luckie, D.B., Van Alst, A.J., Massey, M.K., Flood, R.D., Shah, A.A., Malhotra, V., et al. 2014. Chemical rescue of DeltaF508-CFTR in C127 epithelial cells reverses aberrant extracellular pH acidification to wild-type alkalization as monitored by microphysiometry. Biochem. Biophys. Res. Commun. **451**(4): 535-540. doi:10.1016/j.bbrc.2014.08.036.

Martel, G., Roussel, L., and Rousseau, S. 2013. The protein kinases TPL2 and EGFR contribute to ERK1/ERK2 hyperactivation in CFTRDeltaF508-expressing airway epithelial cells exposed to Pseudomonas aeruginosa. Biochem. Biophys. Res. Commun. **441**(3): 689-692. doi:10.1016/j.bbrc.2013.10.030.

Martinez, D., Vermeulen, M., von Euw, E., Sabatte, J., Maggini, J., Ceballos, A., et al. 2007. Extracellular acidosis triggers the maturation of human dendritic cells and the production of IL-12. J. Immunol. **179**(3): 1950-1959. doi:10.4049/jimmunol.179.3.1950.

Massip-Copiz, M., Clauzure, M., Valdivieso, A.G., and Santa-Coloma, T.A. 2018. Epiregulin (EREG) is upregulated through an IL-1beta autocrine loop in Caco-2 epithelial cells with reduced CFTR function. J. Cell. Biochem. **119**(3): 2911-2922. doi:10.1002/jcb.26483.

Massip-Copiz, M.M., and Santa-Coloma, T.A. 2018. Extracellular pH and lung infections in cystic fibrosis. Eur. J. Cell Biol. **97**(6): 402-410. doi:10.1016/j.ejcb.2018.06.001.

Massip-Copiz, M.M., Clauzure, M., Valdivieso, A.G., and Santa-Coloma, T.A. 2017. CFTR impairment upregulates c-Src activity through IL-1beta autocrine signaling. Arch. Biochem. Biophys. **616**: 1-12. doi:10.1016/j.abb.2017.01.003.

Massip Copiz, M.M., and Santa Coloma, T.A. 2016. c- Src and its role in cystic fibrosis. Eur. J. Cell Biol. **95**(10): 401-413. doi:10.1016/j.ejcb.2016.08.001.

Matrisian, L.M., Rautmann, G., Magun, B.E., and Breathnach, R. 1985. Epidermal growth factor or serum stimulation of rat fibroblasts induces an elevation in mRNA levels for lactate dehydrogenase and other glycolytic enzymes. Nucleic Acids Res. **13**(3): 711-726. doi:10.1093/nar/13.3.711.

McShane, D., Davies, J.C., Davies, M.G., Bush, A., Geddes, D.M., and Alton, E.W. 2003. Airway surface pH in subjects with cystic fibrosis. Eur. Respir. J. **21**(1): 37-42. doi:10.1183/09031936.03.00027603.

Meyer, K.C., Amessoudji, A., Hollatz, T., and Tsao, F.H.S. 2018. Lactic acid concentrations in bronchoalveolar lavage fluid correlate with neutrophil influx in cystic fibrosis. Arch Biomed Clin Res **1**(1): 1-4. doi:10.15761/ABCR.1000101.

Mishra, D., and Banerjee, D. 2019. Lactate Dehydrogenases as Metabolic Links between Tumor and Stroma in the Tumor Microenvironment. Cancers (Basel) **11**(6): 750. doi:10.3390/cancers11060750.

Ogilvie, V., Passmore, M., Hyndman, L., Jones, L., Stevenson, B., Wilson, A., et al. 2011. Differential global gene expression in cystic fibrosis nasal and bronchial epithelium. Genomics **98**(5): 327-336. doi:10.1016/j.ygeno.2011.06.008.

Osherov, N., and Levitzki, A. 1994. Epidermal-growth-factor-dependent activation of the src-family kinases. Eur. J. Biochem. **225**(3): 1047-1053. doi:10.1111/j.1432-1033.1994.1047b.x.

Polineni, D., Dang, H., Gallins, P.J., Jones, L.C., Pace, R.G., Stonebraker, J.R., et al. 2018. Airway Mucosal Host Defense Is Key to Genomic Regulation of Cystic Fibrosis Lung Disease Severity. Am. J. Respir. Crit. Care Med. **197**(1): 79-93. doi:10.1164/rccm.201701-0134OC.

Rice, A.B., Moomaw, C.R., Morgan, D.L., and Bonner, J.C. 1999. Specific inhibitors of platelet-derived growth factor or epidermal growth factor receptor tyrosine kinase reduce pulmonary fibrosis in rats. Am. J. Pathol. **155**(1): 213-221. doi:10.1016/s0002-9440(10)65115-2.

Riordan, J.R. 2008. CFTR function and prospects for therapy. Annu. Rev. Biochem. **77**: 701-726. doi:10.1146/annurev.biochem.75.103004.142532.

Riordan, J.R., Rommens, J.M., Kerem, B., Alon, N., Rozmahel, R., Grzelczak, Z., et al. 1989. Identification of the cystic fibrosis gene: cloning and characterization of complementary DNA. Science **245**(4922): 1066-1073. doi:10.1126/science.2475911.

Sambrook J, F.E., Maniatis T. 1989. Molecular Cloning, a laboratory manual. New York.

Sermet-Gaudelus, I., Vallée, B., Urbin, I., Torossi, T., Marianovski, R., Fajac, A., et al. 2002. Normal function of the cystic fibrosis conductance regulator protein can be associated with homozygous (Delta)F508 mutation. Pediatr. Res. **52**(5): 628-635. doi:10.1203/00006450-200211000-00005.

Shah, V.S., Meyerholz, D.K., Tang, X.X., Reznikov, L., Abou Alaiwa, M., Ernst, S.E., et al. 2016. Airway acidification initiates host defense abnormalities in cystic fibrosis mice. Science **351**(6272): 503-507. doi:10.1126/science.aad5589.

Shamsuddin, A.K., and Quinton, P.M. 2014. Native small airways secrete bicarbonate. Am. J. Respir. Cell Mol. Biol. **50**(4): 796-804. doi:10.1165/rcmb.2013-0418OC.

Shi, Z., Tiwari, A.K., Shukla, S., Robey, R.W., Kim, I.W., Parmar, S., et al. 2009. Inhibiting the function of ABCB1 and ABCG2 by the EGFR tyrosine kinase inhibitor AG1478. Biochem. Pharmacol. **77**(5): 781-793. doi:10.1016/j.bcp.2008.11.007.

Shoshani, T., Augarten, A., Gazit, E., Bashan, N., Yahav, Y., Rivlin, Y., et al. 1992. Association of a nonsense mutation (W1282X), the most common mutation in the Ashkenazi Jewish cystic fibrosis patients in Israel, with presentation of severe disease. Am. J. Hum. Genet. **50**(1): 222-228.

Simonin, J., Bille, E., Crambert, G., Noel, S., Dreano, E., Edwards, A., et al. 2019. Airway surface liquid acidification initiates host defense abnormalities in Cystic Fibrosis. Sci. Rep. **9**(1): 6516. doi:10.1038/s41598-019-42751-4.

Sopper, D.S. 2019. Significance of the Difference between Two Slopes Calculator [Software v 4.0]. Available from danielsoper.com/statcalc.

Stolarczyk, M., and Scholte, B.J. 2018. The EGFR-ADAM17 Axis in Chronic Obstructive Pulmonary Disease and Cystic Fibrosis Lung Pathology. Mediators Inflamm. **2018**: 1067134. doi:10.1155/2018/1067134.

Stolarczyk, M., Veit, G., Schnur, A., Veltman, M., Lukacs, G.L., and Scholte, B.J. 2018. Extracellular oxidation in cystic fibrosis airway epithelium causes enhanced EGFR/ADAM17 activity. Am. J. Physiol. Lung Cell Mol. Physiol. **314**(4): L555-L568. doi:10.1152/ajplung.00458.2017.

Sun, X., Liang, J., Yao, X., Lu, C., Zhong, T., Hong, X., et al. 2015. The activation of EGFR promotes myocardial tumor necrosis factor-alpha production and cardiac failure in endotoxemia. Oncotarget **6**(34): 35478-35495. doi:10.18632/oncotarget.6071.

Takai, N., Ueda, T., Nishida, M., Nasu, K., and Narahara, H. 2010. Synergistic anti-neoplastic effect of AG1478 in combination with cisplatin or paclitaxel on human endometrial and ovarian cancer cells. Mol Med Rep **3**(3): 479-484. doi:10.3892/mmr_00000284.

Taminelli, G.L., Sotomayor, V., Valdivieso, A.G., Teiber, M.L., Marin, M.C., and Santa-Coloma, T.A. 2008. CISD1 codifies a mitochondrial protein upregulated by the CFTR channel. Biochem. Biophys. Res. Commun. **365**(4): 856-862. doi:10.1016/j.bbrc.2007.11.076.

Tate, S., MacGregor, G., Davis, M., Innes, J.A., and Greening, A.P. 2002. Airways in cystic fibrosis are acidified: detection by exhaled breath condensate. Thorax **57**(11): 926-929. doi:10.1136/thorax.57.11.926.

Valdivieso, A.G., and Santa-Coloma, T.A. 2013. CFTR activity and mitochondrial function. Redox Biol **1**(1): 190-202. doi:10.1016/j.redox.2012.11.007.

Valdivieso, A.G., and Santa-Coloma, T.A. 2019. The chloride anion as a signalling effector. Biol. Rev. Camb. Philos. Soc. **94**(5): 1839-1856. doi:10.1111/brv.12536.

Valdivieso, A.G., Clauzure, M., Massip-Copiz, M., and Santa-Coloma, T.A. 2016. The Chloride Anion Acts as a Second Messenger in Mammalian Cells - Modifying the Expression of Specific Genes. Cell. Physiol. Biochem. **38**(1): 49-64. doi:10.1159/000438608.

797 Valdivieso, A.G., Mori, C., Clauzure, M., Massip-Copiz, M., and Santa-Coloma, T.A. 2017. CFTR
798 modulates RPS27 gene expression using chloride anion as signaling effector. Arch. Biochem.
799 Biophys. **633**: 103-109. doi:10.1016/j.abb.2017.09.014.
800
801 Valdivieso, A.G., Clauzure, M., Massip-Copiz, M.M., Cancio, C.E., Asensio, C.J.A., Mori, C., et al.
802 2019. Impairment of CFTR activity in cultured epithelial cells upregulates the expression and
803 activity of LDH resulting in lactic acid hypersecretion. Cell. Mol. Life Sci. **76**(8): 1579-1593.
804 doi:10.1007/s00018-018-3001-y.
805
806 Valdivieso, A.G., Marcucci, F., Taminelli, G., Guerrico, A.G., Alvarez, S., Teiber, M.L., et al. 2007.
807 The expression of the mitochondrial gene MTND4 is downregulated in cystic fibrosis. Biochem.
808 Biophys. Res. Commun. **356**(3): 805-809. doi:10.1016/j.bbrc.2007.03.057.
809
810 Valdivieso, A.G., Clauzure, M., Marin, M.C., Taminelli, G.L., Massip Copiz, M.M., Sanchez, F., et
811 al. 2012. The mitochondrial complex I activity is reduced in cells with impaired cystic fibrosis
812 transmembrane conductance regulator (CFTR) function. PLoS One **7**(11): e48059.
813 doi:10.1371/journal.pone.0048059.
814
815 Veit, G., Avramescu, R.G., Chiang, A.N., Houck, S.A., Cai, Z., Peters, K.W., et al. 2016. From CFTR
816 biology toward combinatorial pharmacotherapy: expanded classification of cystic fibrosis
817 mutations. Mol. Biol. Cell **27**(3): 424-433. doi:10.1091/mbc.E14-04-0935.
818
819 Voskuil, F.J., Steinkamp, P.J., Zhao, T., van der Vegt, B., Koller, M., Doff, J.J., et al. 2020.
820 Exploiting metabolic acidosis in solid cancers using a tumor-agnostic pH-activatable nanoprobe
821 for fluorescence-guided surgery. Nature Communications **11**(1): 3257. doi:10.1038/s41467-020-
822 16814-4.
823

824 Worlitzsch, D., Döring, G., Kottmann, R., Phipps, R., and Sime, P. 2013. Lactate Levels in Airways
825 of Patients with Cystic Fibrosis and Idiopathic Pulmonary Fibrosis. Am. J. Respir. Crit. Care Med.
826 **188**(1): 111. doi:10.1164/rccm.201211-2042LE.
827
828 Yang, Q., Soltis, A.R., Sukumar, G., Zhang, X., Caohuy, H., Freedy, J., et al. 2019. Gene therapy-
829 emulating small molecule treatments in cystic fibrosis airway epithelial cells and patients. Respir.
830 Res. **20**(1): 290. doi:10.1186/s12931-019-1214-8.
831
832 Zeitlin, P.L., Lu, L., Rhim, J., Cutting, G., Stetten, G., Kieffer, K.A., et al. 1991. A cystic fibrosis
833 bronchial epithelial cell line: immortalization by adeno-12-SV40 infection. Am. J. Respir. Cell
834 Mol. Biol. **4**(4): 313-319. doi:10.1165/ajrcmb/4.4.313.
835
836
837 **Figure legends**

838 **Figure 1. The impairment of the CFTR activity in IB3-1 cells decreases the extracellular pH,**
839 **increases LDH activity, and lactic acid secretion.** IB3-1 (CF cells) and C38 cells (IB3-1 "rescued"
840 cells) were incubated in serum-free medium and the pHe measured. (A) pHe values in the conditioned
841 media after 48 h. (B) Lactic acid concentration in conditioned media from IB3-1 and C38 cells,
842 measured as lactate, after 48 h of incubation. (C) Lactic acid concentration in conditioned from IB3-
843 1 cells (black line) and C38 cells (gray line), at 0, 24, and 48 h, measured as lactate. The results were
844 fitted using linear regression. The slopes are shown and had a significant difference ($p < 0.05$, n=3).
845 * indicates significant differences compared to the untreated cells. (D) Intracellular LDH activity in
846 IB3-1 and C38 cells, measured after 48 h of incubation in serum-free medium; the values of C38 was
847 normalized to 100 % of activity. * indicates $p < 0.05$. IB3-1 cells show a significant reduction in
848 pHe, in conditioned media.

849 **Figure 2. EGFR inhibitors normalized the pHe of IB3-1 cells.** IB3-1 and C38 cells were cultured
850 in serum-free medium in the presence of EGFR inhibitors and the pHe was measured at 48 h. (A)

Dose-response curve corresponding to pHe measured in conditioned media from IB3-1 cells treated with different concentrations of the EGFR inhibitor AG1478; ED_{50} = 5.9 ± 0.3 μM. (B) Dose-response curve of IB3-1 cells treated with the EGFR inhibitor PD168393; ED_{50} = 2.1 ± 0.5 μM. The dose-response curves were fitted by using a sigmoidal function. (C) IB3-1 and C38 cells incubated with 10 μM AG1478. (D) IB3-1 and C38 cells incubated with 10 μM PD168393. * indicates $p < 0.05$.

Figure 3. LDH activity and lactic acid secretion are modulated by EGFR inhibitors. IB3-1 and C38 cells were cultured in serum-free medium in the presence of EGFR inhibitors. (A) Intracellular LDH activity in C38 and IB3-1 cells treated with the EGFR inhibitor AG1478 (10 μM). LDH activity was expressed as %, normalized to C38 as 100% activity. (B) Cells were incubated with the EGFR inhibitor PD168393 (10 μM). (C) Lactate concentration in conditioned media of IB3-1 cells treated with AG1478 at 0, 24, and 48 h. (D) Lactate concentration in conditioned media of IB3-1 cells treated with PD168393 at 0, 24, and 48 h. * indicates $p < 0.05$.

Figure 4. LDHA expression is upregulated in CF-cells. IB3-1 and C38 cells were incubated 48 h in serum-free medium. After incubation, total proteins or total RNA were extracted and the LDHA protein levels and *LDHA* mRNA were determined by WB or real-time PCR. The same treatment was applied to measure LDHA and p-LDHA by using flow cytometry. (A) Quantitative real-time RT-PCR of *LDHA* mRNA expression levels in C38 and IB3-1 cells. (B) Representative WB corresponding to LDHA and p-LDHA from whole-cell lysates of C38 and IB3-1 cells. (C) Densitometric quantification of p-LDHA/actin (D) Densitometric quantification of LDHA/actin. (E) Confocal image of LDHA in C38 and IB3-1 cells; (a) confocal fluorescent image with anti LDHA antibodies (b) visible transmitted light image. (F) Representative cytometry of LDHA expression. (G) average MFI (mean fluorescence intensity) values of F. (H) Representative cytometry of p-LDHA expression. (I) MFI average values of data in H. MFI values are normalized to control values. *indicates $p < 0.05$.

Figure 5. LDHA expression is modulated by EGFR inhibitors. IB3-1 cells were incubated 48 h in serum-free medium and treated with EGFR inhibitors (AG1478 and PD168393). After incubation, total RNA was extracted and the LDHA mRNA was determined by real-time PCR. Alternatively, cells were collected and fixed with paraformaldehyde 4% to measure LDHA expression by flow cytometry by using the anti-LDHA Ab. (A) Quantitative real-time RT-PCR of LDHA mRNA expression levels in IB3-1 cells. (B) LDHA expression is shown as mean fluorescence intensity (MFI) and normalized to control values. *indicates $p < 0.05$. (C) Representative dot plots of the cytometries shown in B. FL1-A (fluorescence intensity in the green channel) vs FSC-A (forward scattering). Plots are shown for IB3-1 cells treated with the EGFR inhibitors AG1478 and PD168393, respectively. *indicates $p < 0.05$.

Figure 6. Graphic summary. The figure summarizes the pathways and interactions involved in the results obtained here. It is just a working model to illustrate the interactions known so far. Several interactions need further studies, in particular the intermediary effectors downstream of EGFR that stimulate both, the LDHA expression and regulation by phosphorylation. The impairment of the CFTR activity induces chloride accumulation that, acting as a second messenger, starts an autocrine IL-1β loop, with stimulated c-Src and JNK activities that modulate the secretion of lactate {Valdivieso, 2019 #1129}. Here, EGFR seems to be an important player in regulating lactate secretion. The activated EGFR in IB3-1 cells resulted in a higher LDH activity and production of lactate, which is secreted (together with H^+), reducing the extracellular pH (pHe). The signaling mechanism between CFTR and EGFR, which includes Cl^-, c-Src, IL-1β, and EGFR ligands are still ill-defined (dotted line). These results were obtained using IB3-1 lung epithelial CF cells *in vitro* and may differ from results obtained *in vivo* or expressed only under stress conditions (infections or injured tissues).

900 **Figures**

901

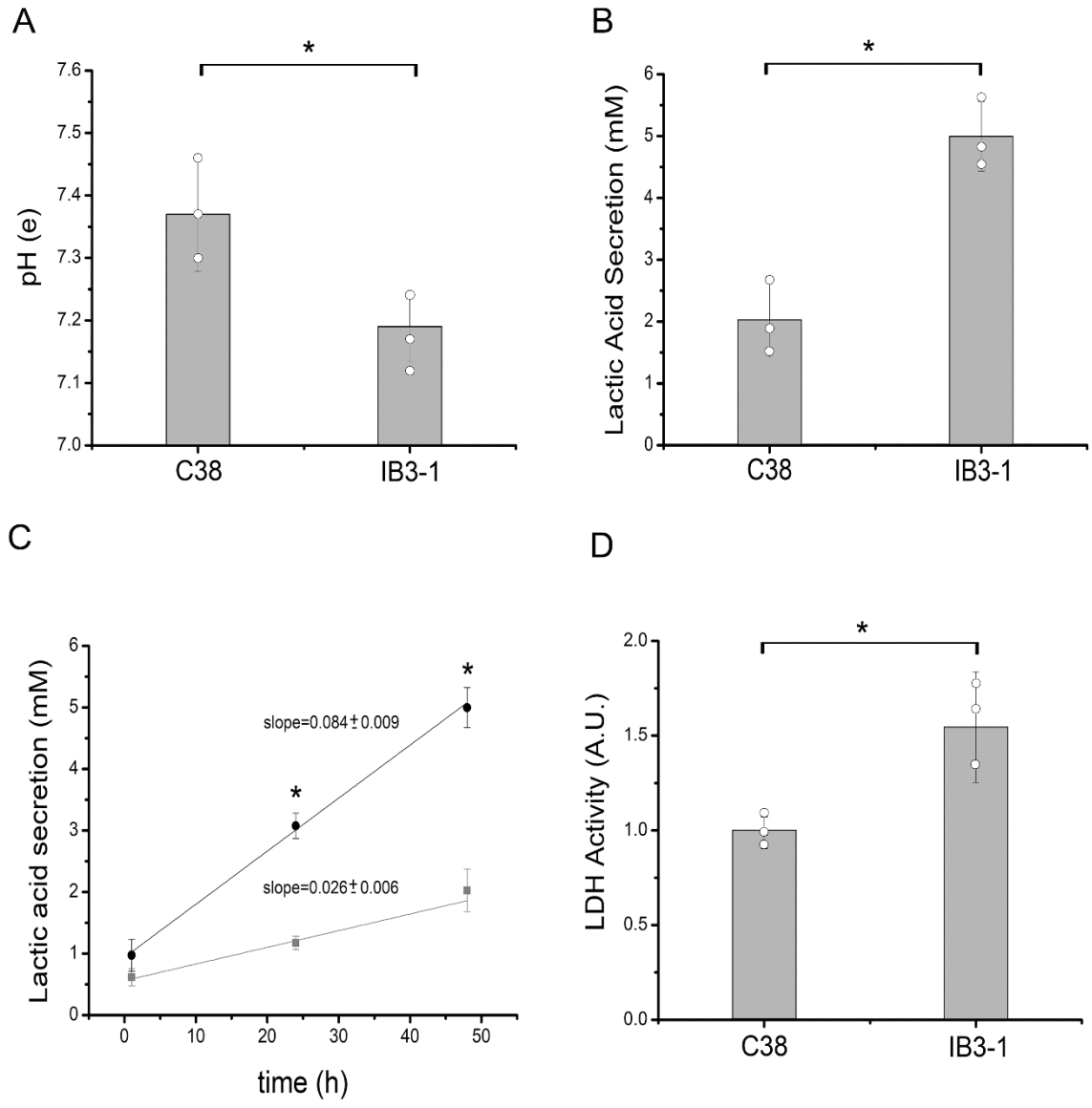

902

903 **Figure 1**

904

905

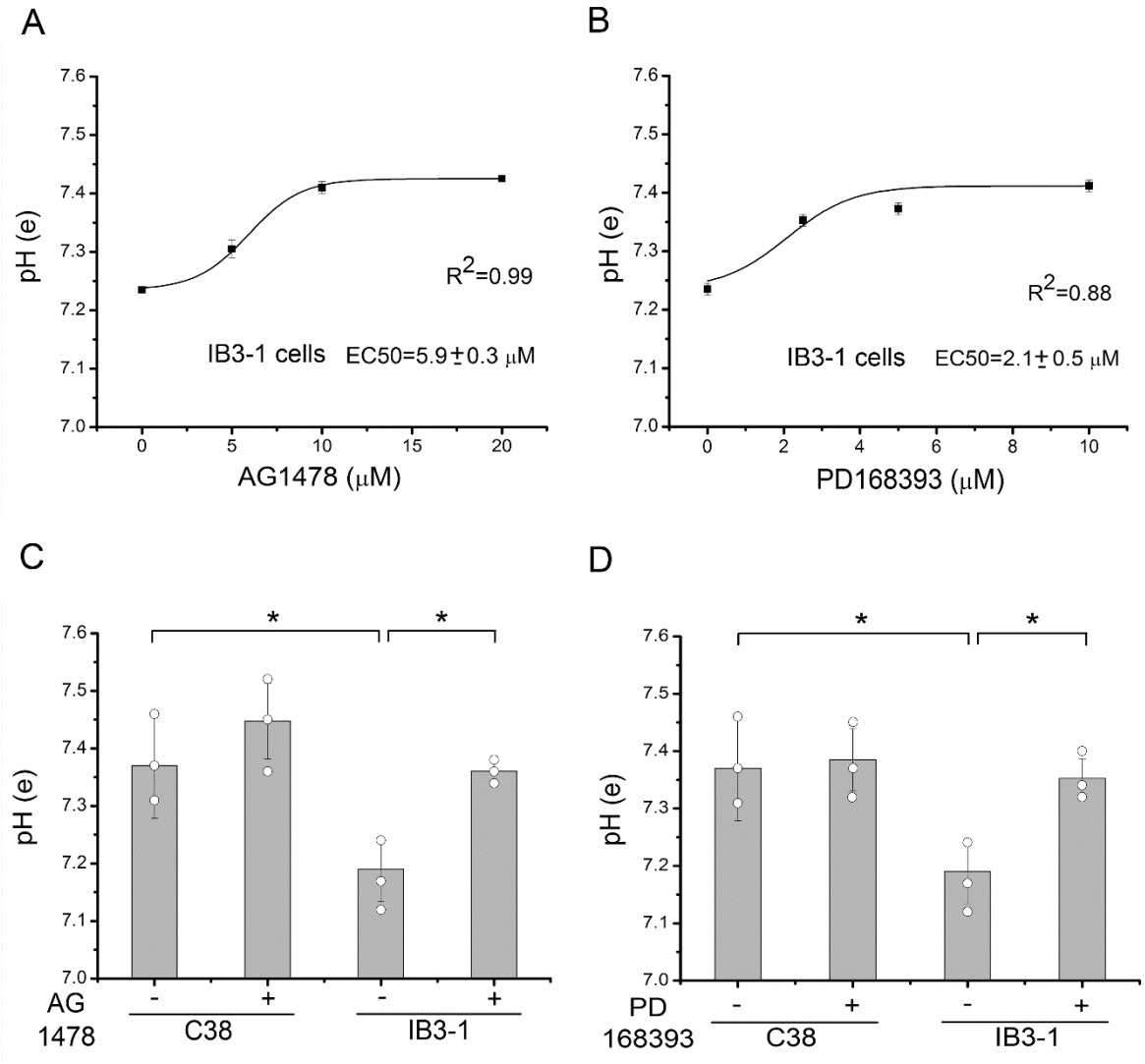

906

907

908 **Figure 2**

909

910

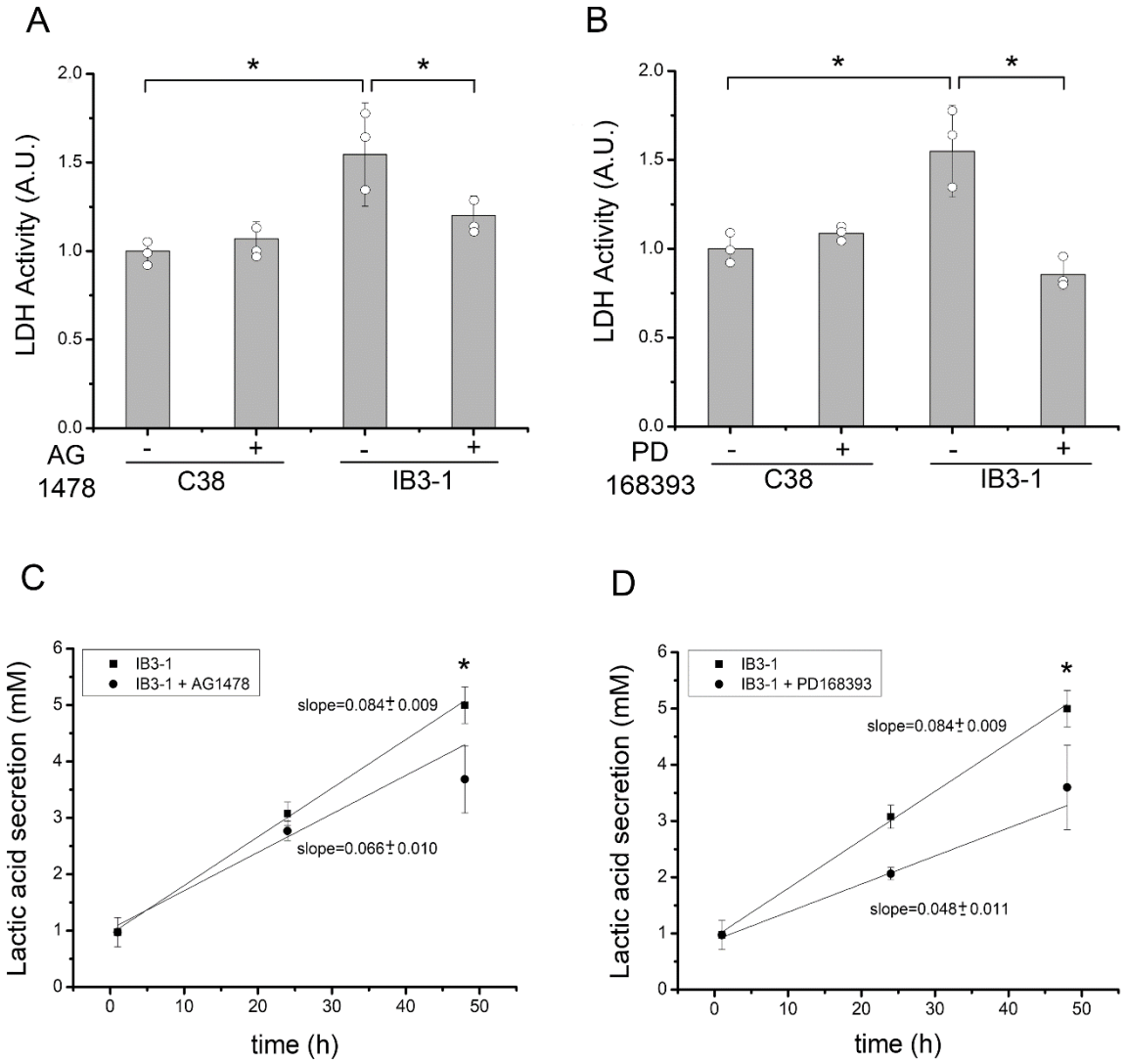

911

912

913 **Figure 3**

914

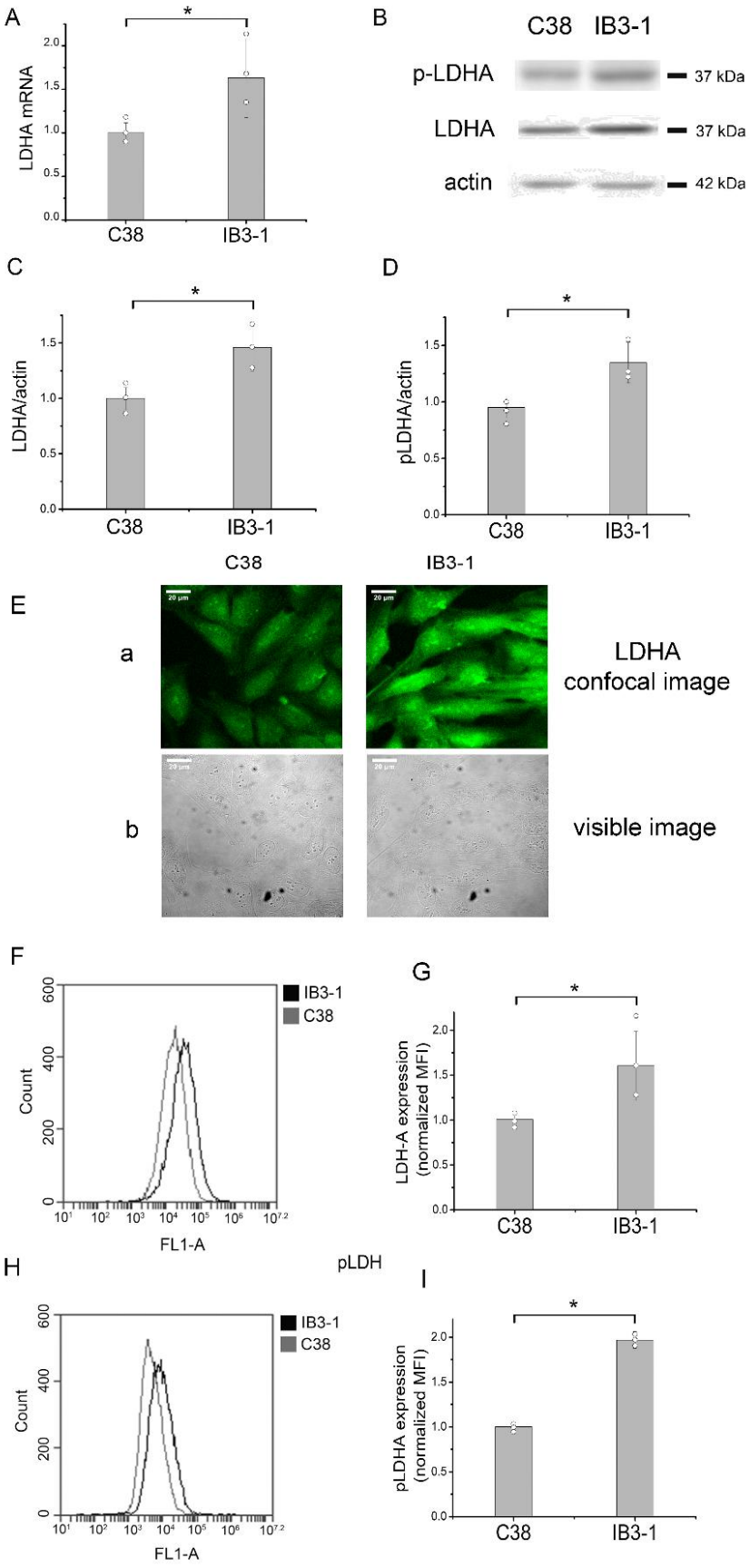

915

916 **Figure 4**

Figure 5

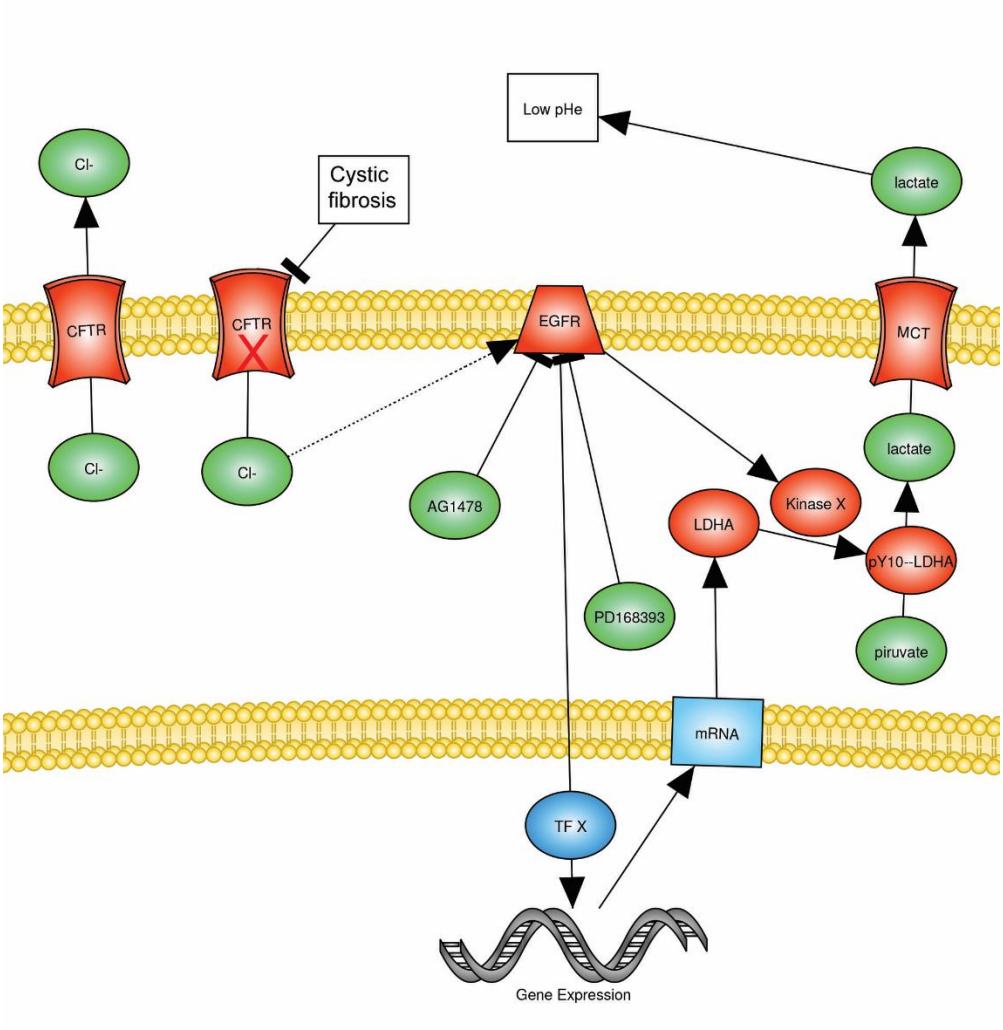

924

925 **Figure 6**